Proc. of the 2018 International Symposium on Electromagnetic Compatibility (EMC Europe 2018), Amsterdam, The Netherlands, August 27−30, 2018.

# Automated Filter Optimization for High-Voltage Cable Harness based on Circuit Simulations for Conducted Emissions Prediction

Denis Mueller*, M.Beltle, S. Tenbohlen
Institute of Power Transmission and High Voltage Technology
University of Stuttgart, Germany
*denis.mueller@ieh.uni-stuttgart.de

*Abstract*—**EMI suppression in vehicles cable harnesses is commonly realized by passive EMI filters. Rising battery voltages, faster semiconductor switches and the use of unshielded DC-cables requires larger filters. In addition, it is necessary being able to estimate the size of the EMI-filter in an early stage of development, when no measurements of the conducted emissions exist yet. To solve this problem, an automated filter optimization tool based on simulations for the prediction of conducted common-mode emissions (CE) is presented. The simulation model requires only a little information of the inverter which is accessible at an early stage of development. The accuracy of the model is good enough to predict the CE up to 30 MHz. In combination with a differential evolution algorithm for the optimization of the filters components, a fast estimation of the required space can be achieved.**

***Keywords—EMC; Electromagnetic Compatibility; EMI; Automated Filter Design; Differential Evolution; Common Mode Suppression***

## I. Introduction

The use of wide bandgap semiconductors in traction inverters for electrical vehicles offers clear advantages in terms of the required installation space compared to conventional semiconductor technologies. These new semiconductor substrates enable steep-flanked switching processes, high blocking voltages and high clock rates, but at the cost of increased interference potential. At the same time, weight and costs have to be minimized by using unshielded DC cables and increasing the DC voltage up to 800 V. For these reasons, the dimensioning of the necessary EMI-filters must be larger, which puts the installation space advantage into perspective. In some cases, EMC filter assemblies require up to 40% of the total installation space of an inverter [1]. These mechanisms lead to increasingly tougher demands on filter assemblies in terms of insertion loss, cost and weight. The aim of the development is to design a filter that is as compact and efficient as possible but also provides the necessary insertion loss for suppressing disturbances from the traction inverter.

Typically, measurements are needed to develop the required EMI-Filter. To deliver these information without having measurements of the inverter prototype, simulations with different degrees of complexity are created. The first stage of such models are simple circuit simulations. In this case no information of the geometry of the inverter is required and a first estimation of the conducted disturbance voltage can be done [2]. The second stage is a detailed 3D geometry simulation. Both simulation models are verified using measurements from a CISPR25 setup on an inverter and filter prototype [2]. In order to apply circuit simulations for the optimization of a filter in the system network, an optimization algorithm is presented, which includes the conducted disturbance voltage from a simulation into the optimization process. Based on this simulation, the algorithm provides an optimized selection of components in order to achieve the necessary insertion loss, but not to oversize the system at the same time. In order to validate the method, a filter is designed based on an application example and optimized by means of the presented algorithm, which is measured in the lab setup and thus the suitability of the algorithm is confirmed. With such a simulation based optimization algorithm a first estimation of the filters installation space in an early stage of development can be done.

## II. Optimization Based on Disturbance Voltage Simulation

### A. Conventional Filter Design

Conventional filters are often designed in an iterative process in which, for example, the capacitors $C_Y$ are designed for common-mode suppression according to the maximum permissible leakage currents. If their values are fixed, the resonance point of common mode choke and $C_Y$ capacitors is selected in such a way that the maximum required insertion loss is guaranteed [1], [3].

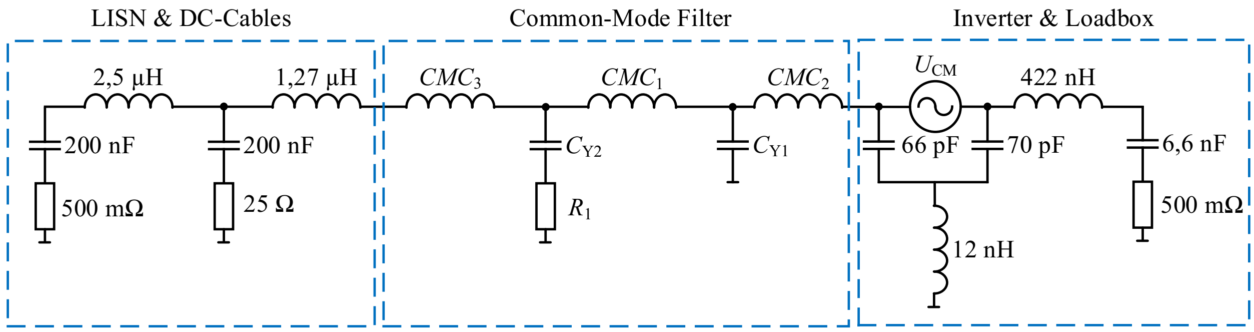


Fig. 1. Single-phase equivalent circuit of the circuit simulation SPICE model with included common mode filter

However, the disadvantage of this design method is that the selected combination of capacitors and common mode choke does not necessarily represent the most efficient solution with regard to costs expenditure. Also the final filter is only available after several iterations with measurements. Out of this disadvantage, [1] describes the optimization of EMI-Filter mass by automated based on simulations. A number of methods for automatic filter optimization using software tools have been introduced in the past [3]-[8]. Most optimization processes are based on measurements of the unfiltered system to determine the necessary filter attenuation [3]-[7]. The differences between these tools are the used optimization algorithms, for example rule based [3] or particle swarm optimization [4], and the accuracy of the filter model. These models predict the filters attenuation, size and costs with a high degree of accuracy, which is necessary at an advanced development stage. However, at an early stage of development it is often needed to estimate the EMI filter without having the required measurements of prototypes. Therefore, a method is to be presented that allows the automated and simulation-based design of an optimized filter in a few minutes without measurements. In this way, the oversizing of the filter components can be avoided. Later, in the advanced development process, when measurements of the inverters disturbances and complex models are available, detailed optimization tools can be used to calculate the final EMI filter.

## *B. Use of Circuit Simulations for Filter Design*

In [8] the possibility of a design accompanying circuit simulation for predicting the disturbance voltage at the line impedance stabilization network (LISN) is presented. This approach allows a parallel development of filters during the design phase of the inverter, which can simplify the integration of this module into the complete inverter considerably. By combining the simulation with a suitable optimization algorithm, the minimum required filter component can be calculated before the sample phase starts, which can save iterations and thus reduce development costs.

Fig. 1 shows the common mode equivalent circuit presented in [9], extended with the single-phase representation of a common mode filter. The equivalent circuit consists of the common-mode equivalents of line impedance stabilization network (LISN) and DC cables (left), inverter and three phase load (right) and is supplemented additionally by the common-mode filter, which consists of the common-mode chokes ($CMC_{1,2,3}$), common-mode capacitors ($C_{Y1,\ Y2}$) and a damping resistor $R_1$. This common-mode model is implemented in a frequency domain SPICE simulation. As common-mode stimulation the source $U_{CM}$ is used, their voltage follows the envelope of the spectrum of the MOSFETs voltages. This spectrum can be obtained by measuring the switch voltage during the switching process of the MOSFET followed by Fast Fourier Transformation (FFT). It is also possible to estimate the required information, only based on the battery voltage and switching frequency [2]. The corresponding component values, such as the parasitic capacitance and inductance of the LISN, cables and loadbox can be obtained also by measurements using the setup according to CISPR25 component test and are available at an early stage of development. Since the equivalent circuit diagram can be used to simulate the disturbance voltage at the BNN with sufficient accuracy [2], it is intended to demonstrate that filter optimization can be carried out under realistic impedance conditions.

Fig. 2 shows the measured disturbance voltage at the LISN compared to the prediction of the circuit simulation. The deviation between simulated envelope of the spectrum and measurement is smaller than 1 dB up to 10 MHz. Up to 30 MHz the deviation is smaller than 3 dB, only the resonance at 25 MHz is not distinct in the measurement.

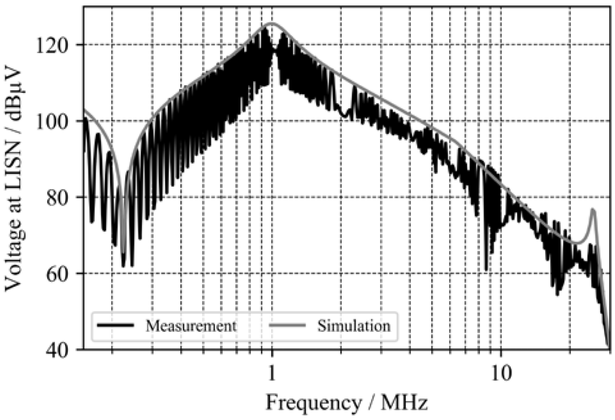


Fig. 2. Conducted emission of an inverter in CISPR25 test setup compared to the circuit simulation in Fig. 1

This high accuracy model in the lower frequency range can be simulated on an ordinary PC within seconds. Hence, it is considered as a good basis for heuristic optimization.

## III. Development and Implementation of the Algorithm

The optimization of the common mode filter can be separated into two sub-problems: The optimization of the components costs and the dimensioning of the filter according of the specified limit of the acceptable disturbance voltage. In order to design the correct filter, the algorithm must include both sub-problems in the optimization process. Heuristic search methods such as Evolutionary Algorithms or Particle Swarm Optimization are considered suitable for this task [4], [8]. These algorithms are based on the iterative, targeted enhancement of a set of randomly generated solution vectors. In order to include the disturbance voltage simulation efficiently in the optimization, an interface has to be implemented in the algorithm which incorporates the SPICE solver to this simulation. The algorithm is implemented in MATLAB without using the optimization toolbox. If the algorithm should be used in another case, the source code is enclosed in such a way that only a suitable simulation model has to be stored, the parameters, their limits and the target function need to be adapted. As long as the simulation should be calculated in frequency domain, there is no change in the algorithms source code necessary. Due to good convergence characteristics, a Differential Evolution algorithm, a subspecies of Genetic Algorithms, is chosen for problem solving [10]. [11] and [12] show that Differential Evolution convergents faster than Particle Swarm Optimization and in [13] Differential Evolution turns out to be very robust against different initial conditions. To be able to deal with different types of problems without deep changings, a robust algorithm is required, wherefore the Differential Evolution Algorithm was chosen.

### A. *Differential Evolution Algorithm*

Generally, Genetic Algorithms are based on the principle of evolution. The Differential Evolution algorithm is a subtype of this group of algorithms. The sequence diagram in Fig. 3 shows the optimization process according to the Differential Evolution algorithm. At the beginning, a random initial population of individuals, the "parent" population, which represents possible solution vectors, is generated from a previously defined solution space and then subjected to a recombination step. A solution vector could be a combination of filter elements for example. The individual values of the solution vectors are manipulated according to a defined recombination formula and thus new solution vectors, the "child" population, are generated. The problem to be optimized is represented by a function on the basis of which the functional values of the individuals, the fitness, which e.g. corresponds with the costs, can be calculated. In a selection step, the parent and child population are listed according to their fitness and a certain amount of solution candidates with the worst fitness, the highest functional value, are deleted. The remaining population is then returned to the recombination step and the process will be repeated.

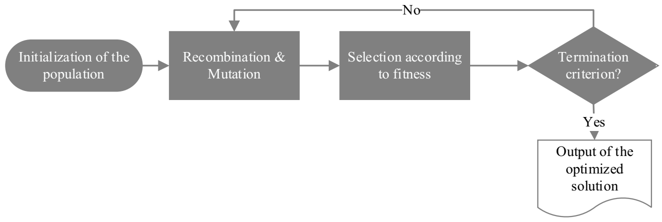


Fig. 3. Sequence diagram of the typical differential evolution algorithm

With each pass, the fitness of the entire population is increased, bringing the solution vectors closer to an local optimum. The accuracy of the optimization can be determined using a defined termination criterion. The result of this procedure represents a local optimum of the defined fitness function.

### B. *Implementation of Disturbance Voltage Simulation*

In order to understand the structure of the developed algorithm, it is necessary to know the fitness evaluation of the individuals. In this case, an individual is a combination of component values from a given filter topology that represents one possible solution. The fitness rating is done in two steps based on the evaluation of the disturbance voltage simulation. In the first step a defined limit for conducted emissions can be set. Each created individual is fed into the circuit simulation and the simulated disturbance voltage is used for the first evaluation stage. The simulation using the individuals parameter set must comply with the pre-defined limit. If this limit is exceeded, the individual is rejected, otherwise the suitability is given. In the second step costs, installation space or weight are optimized by using the fitness function (3.1). This weights the parameters of the filter with certain factors $K_n$, which, for example, depict the relationship between installation space or costs as a function of the component value.

$$Fitness = K_1 A_{CMC1} + K_2 l_{CMC1} + \ldots + K_{17} C_2 + K_{18} R_1 + K_{19} \quad (3.1)$$

The parameters affecting the fitness function in the current project are the coils cross-section $A$, the average field length of the common-mode choke $l$, the capacitance of the Y-capacitors $C$ and the resistance of the damping resistor $R$. If these factors provide sufficient accuracy, the fitness value directly represents the installation space or the cost of the filter [3]. Due to the lack of data, the weights are generated by a fit of available components prices. Equation (3.2) shows an example for the fit of the capacitors costs.

$$Costs(C) = K_{C4}C^4 + K_{C3}C^3 + K_{C2}C^2 + K_{C1}C + K_{C0} \qquad (3.2)$$

The function fits the capacity dependent costs 'Costs(C)' with a fourth degree polynomial function, where $C$ is the capacitance and $K_{Cn}$ are the coefficients. The resulting cost-function can be used as the part of one Y-capacitor of the fitness-function, to be optimized. The weights of the common-mode choke and the damping resistor where generated in the same way. The fitness function is generated by summing up all components costs.

Fig. 4 shows the sequence diagram extended by the circuit simulations interface. After the first population has been initialized, the simulation will be used to check whether the "parent" population is able to comply with the limit. If this is not the case, the individuals with a limit violation are deleted and new individuals are initialized randomly. This happens until a fixed number of "parent" individuals are found without limit violations and the recombination step can begin. If the number of initial "parents" individuals is to low, the algorithm converges not.

The recombination is based on equation (3.3), where $v$ is the "child" vector, $x$ is the "parent" vector and $R$ is the recombination factor. Since the individuals are always sorted according to their fitness, $j = 1,2,\ldots,N$ represents the rank of the respective vector.

$$v_i = x_1 + R(x_{j+1} - x_{j+2}) \qquad (3.3)$$

The implemented recombination formula is called "DE/best/1/bin". In different publications it showed the fastest convergence of common recombination rules [14]. To create a "child" vector, the difference between two following, random vectors is weighted with the recombination factor and added to the fittest individual. According to equation (3.3), a child population is created whose number of individuals corresponds to the "parent" population. In the first step of the two-step selection, all individuals of the "parent" and "child" vectors are checked for compliance with the limit by simulating the disturbance voltage with SPICE. Individuals that exceed the limit are deleted.

Then the remaining individuals are selected, according to the fitness function (3.1). The worst individuals are deleted until the remaining population has reached the size of the original "parent" population. Since the selected population contains both "parent" and "child" vectors, the total population's fitness improves continuously with each iteration, or stagnates in case of a very weak population. After the selection step, the termination criterion is checked according to (3.4).

$$max\ (y_i - y_{i+1}) < 0{,}01 \qquad (3.4)$$

The maximum difference between the individual solutions of the population is used as a criterion for termination, where $y$ stands for the fitness value of an individual. The condition for the termination criterion has to be adapted depending on the optimization problem. This criterion has turned out to be the best compromise between a fast calculation and good accuracy of the optimized filter.

## IV. Realization of the Filter

The topology selected is a π filter of fifth-order, integrated into the circuit simulation depicted in Fig.1. The single-phase equivalent circuit of the filter is shown in Fig. 5. The model of the common mode chokes ($CMC_{1,2,3}$) is described by the effective cross-sectional $A_{CMC}$, the average field length $l_{CMC}$ in the core and the number of turns $n_{CMC}$.

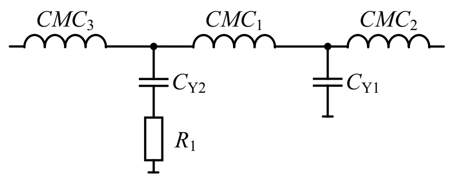


Fig. 5. Single-phase equivalent circuit of the chosen CM-Filter

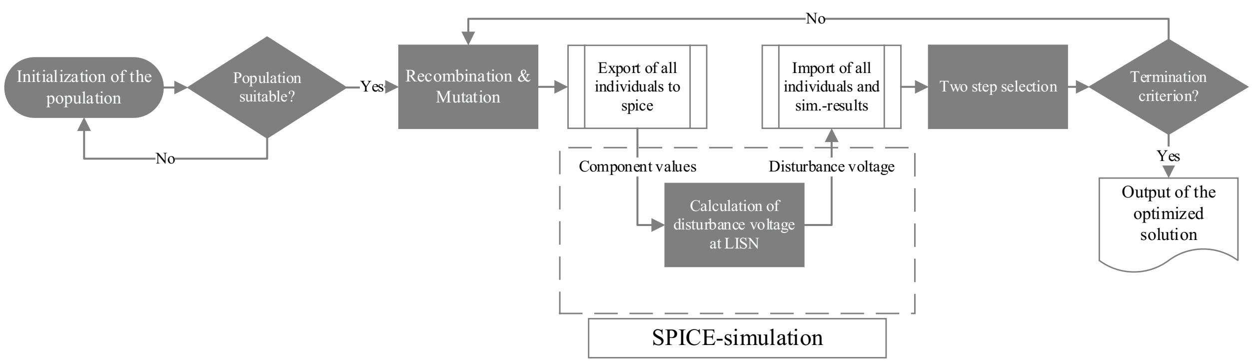


Fig. 4. Single-phase equivalent circuit of the circuit simulation SPICE model with included common mode filter

Capacitors $C_{Y1}$ and $C_{Y2}$ act as Y-capacitors, whereby $C_{Y2}$ is damped with $R_1$ to avoid resonances in the filter. A damping of $C_{Y1}$ is not necessary in the considered frequency range.

### A. Assembly of the Common Mode Filter

The maximum permissible capacitance of 300 nF, is limited by the allowed energy content of the capacitors and taken into account in the boundary conditions of the algorithm. The physical boundary conditions of the common mode choke are commercial dimensions and a maximum number of turns of $n_{CMC} = 2$. The typical currents of electrical vehicle systems do not allow for larger numbers of turns, especially because the winding capacities would limit the performance of the common mode choke at higher.

In order to confirm the result with regard to local optima, several optimization runs with different initial conditions have been carried out. The component values of $C_{Y2}$ and $R_1$ are not relevant for the result due to high dispersion. For the remaining filter elements, a local optimum can be achieved within the search space. The results are shown in Table 1. The largest part of the allowed capacity is allocated to $C_{Y2}$.

TABLE I. RESULTS OF THE OPTIMIZATION ALGORITHM

| Parameter | Optimized value | Parameter | Optimized value |
|---|---|---|---|
| $A_{CMC1}$ | 1.52 cm² | $A_{CMC3}$ | 0.45 cm² |
| $l_{CMC1}$ | 7.8 cm | $l_{CMC3}$ | 6.4 cm |
| $n_{CMC1}$ | 2 | $n_{CMC3}$ | 2 |
| $A_{CMC2}$ | 0.38 cm² | $C_{Y1}$ | 160 nF |
| $l_{CMC2}$ | 7.8 cm | $C_{Y2}$ | 10 nF |
| $n_{CMC2}$ | 1 | $R_1$ | 700 kΩ |

The filter is assembled on a single-layer circuit board, shown in Fig. 6. Nanocrystalline core material is used for the common mode chokes. In order to validate the results of the optimization, a comparison measurement of the conducted interference voltage at the component test according to CISPR25 is performed in the frequency range from 150 kHz to 30 MHz.

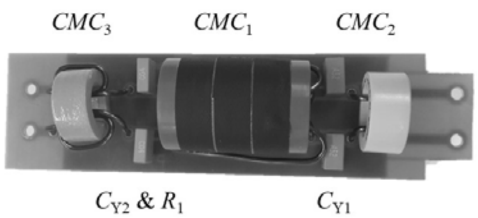


Fig. 6. Assembled common-mode filter

### B. Experimental Validation

Fig. 7 shows the comparison between measurement and simulation of the interference voltage at the LISN. In operation without any filter, the measurement is up to 40 dB above the pre-defined limit. As the simulation shows, the 2 MHz and 3 MHz turns out to be a critical point for limit violations. The comparison of simulation and measurement shows that the actual disturbance voltage at the resonance is 10 dB smaller than estimated by the simulation. With the help of the simulation, this resonance can be traced back to a LC-resonator between the capacity of the machine simulation and the inductance of its connecting cable, which is more damped in the real setup. The deviation between simulation and measurement starting at 7 MHz can be attributed to the frequency behavior of the common mode choke's core material. As measurements show, their permeability decreases with rising frequency to a greater extent than the simulation model represents.

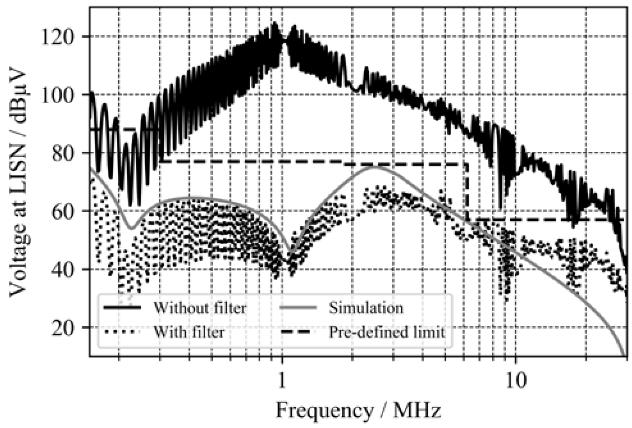


Fig. 7. Conducted emissions of the system according to CISPR25 standard

The experiment shows that even with a strongly simplified model a filter can be realized within minutes, which is cost optimized and complies with a defined limit. This combination of an optimization algorithm and a simple circuit simulation allows an early estimation of the required filter effort, which simplifies the integration into the inverter significantly and avoids potential problems at an early stage. The determined total capacity $C_{Y,filter} = 170$ nF shows that a conventional design of the filter with maximum Y-capacity $C_{max} = 300$ nF would have led to oversizing.

## V. CONCLUSION

Within the scope of the presented study, an optimization tool using a differential evolution algorithm was developed which allows the automated filter design by using a simple circuit simulation. Definable limit values and component limitations can be taken into account and, depending on the complexity of the underlying optimization function, costs, installation space or weight can be optimized simultaneously. Measurements of the optimized filter show that it has a sufficient attenuation, which complies with the specified limit.

This can lead to a shorter construction time for the required filter because the integration into the inverter can take account with the beginning of development.

Difference between the measurement and simulation could be traced back to inaccuracies in the simulation model. More detailed investigations of the used common mode choke models can be carried out to get a better accuracy of the simulation model in frequency ranges above 7 MHz.

The investigated simulation model has only considered common-mode disturbances. This requires the algorithm to be extended by a differential-mode simulation model, which will enable the total filter effort for suppression of the inverters disturbances to be estimated.

## REFERENCES

[1] J.L.Schanen, A. Baraston, M. Delhommais and P. Zanchetta, “Sizing of Power Electronics EMV Filter Using Design by Optimization Methodology”, 7th Power Electronics, Drive Systems & Technologies Conference (PEDSTC’16), Iran University od Science and Technology, Teheran, Iran, 2016, pp. 279-284

[2] P. Hillenbrand, S. Tenbohlen, W. Pfaff and J. Hansen, “EMI Simulation of a Traction Inverter in a CISPR25 Test-Setup”, 7th GMM-Fachtagung, Wolfsburg, Germany, 2017, pp. 43-48

[3] G. Ala, G.C. Giaconia, G. Giglia, M.C. Di Piazza, M. Luna, G. Vitale and P. Zanchetta, “Computer Aided Optimal Design of High Power Density EMI Filters”, IEEE 16th International Conference on Environmental and Electical Engineering (EEEIC’16), Florence, Italy, 2016

[4] F. Viani, F. Robol, M. Salucci and R. Azaro, “Automatic EMI Filter Design Trough Particle Swarm Optimization”, IEEE Trans. on Electromagnetic Compatibility, Vol. 59, No. 4, pp. 1079-1094, August 2017

[5] B. Narayanasamy, H. Janlanbo and F. Luo, “Development of Software to Design Passive Filters for EMI Suppression in SiC DC Fed Motor Drives”, IEEE 3rd Workshop on Wide Bandgap Power Device and Applications (WiPDA), Blacksburg, USA, Nov. 2015, pp. 230-235

[6] D.O. Boillat, F. Krismer and J.W. Kolar, “EMI Filter Volume Minimization of a Three-Phase, Three-Level T-Type PWM Converter System”, IEEE Trans. on Power Electronics, Vol.32, No.4, April 2017, pp. 2473-2480

[7] M.C. Di Piazza, M. Luna, G. Vitale, G. Ala, G.C. Giaconia and G. Giglia, “ODEF: an Interactive Tool for Optimized Design of EMI Filters”, 42nd Annual Conference of the IEEE Industrial Electronics Society (IECON’16), Florence, Italy, Dec. 2016, pp. 5013-5019

[8] S. Singh and B. Singh, “Optimized Passive Filter Design Using Modified Particle Swarm Algorithm for a 12-Pulse Converter-Fed LCI-Synchonous Motor Drive”, IEEE Trans. on Industry Applications, Vol.50, No.4, pp. 2681-2689, July/August 2014

[9] P. Hillenbrand, C. Keller, K. Spanos and S. Tenbohlen, “Understanding Conducted Emissions form an Automotive Inverter Using a Common-Mode Model”, IEEE and EMC Joint Conference, Dresden, Germany, pp. 685-690, August 2015

[10] R. Storn and K. Price, “Differential Evolution – A Simple and Efficient Heuristic for Global Optimization over Continous Spaces, Journal of Global Optimization, 1996

[11] X. Xu and Y. Li, “Comparison between Particle Swarm Optimization, Differential Evolution and Multi-parents Crossover” International Conference on Computiational Intelligence and Security, Harbin, China, 2007, pp. 124-127

[12] J. Vesterstrøm and R. Thomsen, “A Comparative Study of Differential Evolution, Particle Swarm Optimization, and Evolutionary Algorithms on Numerical Benchmark Problems”, Congress on Evolutionary Computation, Vol.2, Portland, OR, USA, 2004, pp. 1980-1987

[13] B. Baus and G.K. Mahanti, “A Comperative Study of Modified Particle Swarm Optimization, Differential Evolution and Artificial Bees Colony Optimization in Synthesis of Circular Array”, International Conference on Power, Control and Embedded Systems (ICPCES), Allahabad, India, 2010, pp. 1-5

[14] Aswani, V.V. Praveen and S. Thangavelu, “Performance Analysis of Variants of Differential Evolution on Mulit-Objective Optimization Problems” Indian Journal of Science and Technology, Vol.8 (17), August 2015